Plasma Science and Technology

PAPER

# Evaluation of influence of cold atmospheric pressure argon plasma operating parameters on degradation of aqueous solution of Reactive Blue 198 (RB-198)

To cite this article: K NAVANEETHA PANDIYARAJ *et al* 2020 *Plasma Sci. Technol.* **22** 055504

 

Plasma Sci. Technol. **22** (2020) 055504 (12pp) https://doi.org/10.1088/2058-6272/ab568d

# Evaluation of influence of cold atmospheric pressure argon plasma operating parameters on degradation of aqueous solution of Reactive Blue 198 (RB-198)

**K NAVANEETHA PANDIYARAJ[1], D VASU[1], P V A PADMANABHAN[1], M PICHUMANI[2], R R DESHMUKH[3] and V KANDAVELU[4]**

[1] Research Division of Plasma Processing (RDPP), Department of Physics, Sri Shakthi Institute of Engineering and Technology, Chinniyam Palayam (post), Coimbatore-641062, India
[2] Department of Nanoscience and Technology, Sri Ramakrishna Engineering College, Coimbatore-641022, India
[3] Department of Physics, Institute of Chemical Technology, Matunga, Mumbai 400019, India
[4] Department of Chemistry, Sri Shakthi Institute of Engineering and Technology, L&T bypass, Chinniyam Palayam (post), Coimbatore-641062, India

E-mail: navaneetharaj@siet.ac.in and dr.knpr@gmail.com

Received 31 July 2019, revised 9 November 2019
Accepted for publication 12 November 2019
Published 19 February 2020

**Abstract**

The intention of this work is to remove Reactive Blue 198 (RB-198) dye components from simulated water solution using cold atmospheric pressure argon plasma jet. Aqueous solutions of RB-198 dye were treated as a function of various operating parameters such as applied potential, reaction time and distance between the plasma jet and surface of the liquid. The efficiency of the degradation of RB-198 molecules was explored by means of UV-Vis spectroscopy. The reactive species involved during the treatment process were examined by optical emission spectra (OES). The present hydroxyl radicals ($OH^{\bullet}$ radical) and hydrogen peroxide ($H_2O_2$) in the plasma-treated aqueous dye solutions were investigated using various spectroscopic techniques. The other parameters such as total organic carbon (TOC), conductivity and pH were also reviewed. The toxicity of plasma-treated RB-198 solution was finally studied by diffusion bacterial analysis and by tracking seed germination processes. The results show that a higher degradation percentage of 99.27% was acquired for the RB-198 treated at higher reaction time and applied potential, and shorter distance between the plasma jet and water surface. This may be due to the formation of various reactive oxygen ($OH^{\bullet}$ radical, atomic oxygen (O) and $H_2O_2$) and nitrogen species (nitric oxide (NO) radicals and $N_2$ second positive system ($N_2$ SPS)) during the processes as confirmed by OES analysis and other spectroscopy analysis. TOC (17.7% – 81.8%) and pH (7.5 – 3.4) values of the plasma-treated RB-198 decreased significantly with respect to various operation parameters, which indicates the decomposition of RB-198 molecules in the aqueous solution. Moreover, the conductivity of plasma-treated RB-198 aqueous solutions was found to have increased linearly during the plasma treatment due to the formation of various ionic species in aqueous solution. The toxicity analysis clearly exhibits the non-toxic behavior of plasma-treated RB-198 aqueous solution towards the bacterial growth and germination of seeds.

Keywords: RB-198, degradation, non-toxicity, cold atmospheric pressure plasma jet

(Some figures may appear in colour only in the online journal)

## 1. Introduction

Nowadays, various dyes (azo, vat, remazol and reactive dyes) are extensively used in textile dyeing as well as other industrial applications such as lasers, solar cells, optical data disks, liquid crystal displays, etc. However, most of the dye molecules are highly toxic in nature, carcinogenic, have low biodegradability and cause serious environmental issues. A major concern in the utilization of dyes in various industries is their degradation to non-toxic compounds while discharging the effluent [1, 2]. According to world statistics, about 15% of dye products are directly dispersed into the environs as dye wastewater, which causes extreme contamination in natural bodies [3]. Currently, Reactive Blue 198 dye (RB-198) is extensively used in the textile industry. However, this dye can be exclusively hydrolyzed in water during the dyeing process and hence most of the dye molecules remain in the discharged effluent. It is important to note that the presence of even a minuscule amount of toxic dye molecules can produce deleterious effects on water ecosystems and adversely affect human health. Moreover, the RB-198 molecules are stable to heat and light and are difficult to destroy. The existence of compounds of dye molecules in surface and groundwater is deliberated as worldwide environmental distress. Moreover, dye molecules have produced some concerning antagonistic effects on human health, including tumors and allergies [4, 5]. Thus, it is important to degrade the organic toxin dye molecules from effluent prior to discharge into the environment.

Nowadays, various treatments such as electrochemical degradation, biodegradation, membrane processing, and adsorption have been developed to treat textile effluents. However, the major limitations of these processes are that they are not economically viable, as they consume more time, energy and materials. Furthermore, the currently employed commercial methods either do not completely remove the toxin molecules or generate secondary toxic products in the effluent creating substantial secondary pollution in the form of sludge, which has to be further treated by another complex procedure before its safe disposal [6–8]. Recent studies have shown that advanced oxidation processes (AOPs) including UV-photocatalysis, ultrasonic cavitation, ozonation, Fenton and photo-Fenton oxidation, plasma and UV/$H_2O_2$ oxidation are promising alternative techniques for toxic organic waste and effluent treatment [9–13].

Among the various AOP techniques, cold atmospheric pressure plasma is of particular interest in the field of effluent treatment because of its unique attributes such as ease of operation, cost-effectiveness, higher degradation efficiency, etc. This process produces various reactive species such as atomic oxygen (O), hydroxyl radicals ($OH^{\bullet}$), hydrogen peroxide ($H_2O_2$), nitric oxide (NO), nitrate ($NO_3^-$), nitrite ($NO_2^-$), etc on gas-liquid interface that has more potential to oxidize and degrade the organic pollutants and hence does not produce any hazardous by-product, which may be formed by other conventional techniques [9–18]. Furthermore, during the treatment, various plasma channels also develop on the water surface, which can attain localized high temperatures within a short span of time, resulting in thermal degradation of the dye molecules. In this work, RB-198 dye was chosen as the simulation wastewater solution. To the best of our knowledge, there have been no reports regarding the degradation of RB-198 using cold atmospheric pressure plasma jet. Hence, the intention of the investigation is to optimize the plasma operating parameters for the degradation of RB-198 molecules from the simulated aqueous solution. The degradation of RB-198 molecules was examined by means of UV–Vis spectroscopy. The optical emission spectra (OES) were used to identify the reactive species that are involved in the reaction. Various spectroscopic methods were used to examine the presence of hydroxyl radicals ($OH^{\bullet}$ radical) and hydrogen peroxide ($H_2O_2$) species in the plasma-treated aqueous solution. The changes in other parameters such as conductivity and pH were also examined. The toxicity of the plasma-treated RB-198 solution was finally studied via diffusion bacterial analysis and examined by tracking seed germination processes.

## 2. Experimental setup and methodology

### 2.1. Materials

RB-198 dye was provided by Junior Exports Pvt Ltd, Tirupur, India. Other chemicals used for characterization were procured from Sigma and Hi-Media, India. Bacteria used for this investigation (*Staphylococcus aureus* (*S. aureus*) and Gram-negative *Escherichia coli* (*E. coli*)) were obtained from Bioline Laboratory, Coimbatore, India.

### 2.2. Plasma treatment

The degradation of RB-198 molecules in aqueous solution was carried out using an AC-excited cold atmospheric pressure plasma reactor. The system comprises a plasma torch, high-frequency (30 kHz) AC power supply with maximum output voltage of 40 kV, gas flow unit and solution container.

Furthermore, the plasma reactor is equipped with an optical emission spectrometer to analyze the reactive species present in the plasma plume. The plasma torch consists of a pin-type cathode made of copper with dimensions of 20 cm (length $l$) × 0.5 cm (diameter $D$). The tip of the cathode is hemispherical in shape. The cathode is shielded by a quartz tube to avoid arcing and a quartz shield was positioned inside another quartz tube with dimensions of 20 cm (length $l$) × 1.1 cm (inner diameter ($D_{\text{inner}}$)) × 1.5 cm (outer diameter ($D_{\text{out}}$)). Another important component of the torch is a copper ring-type ground electrode with dimensions of 1.6 cm of $D_{\text{inner}}$ and 2.5 cm of $D_{\text{out}}$, respectively. The quartz-shielded cathode is placed inside the ring electrode and the distance between both electrodes is adjustable. For this experiment, the distance between them was fixed at 2.5 cm. Finally, in order to avoid the formation of electric induction during the experiment, the whole torch setup was covered by a Teflon enclosure. Finally, an aluminum nozzle was fixed at the exit of the quartz tube. The torch has provision for allowing plasma-forming gas, which is controlled by mass flow

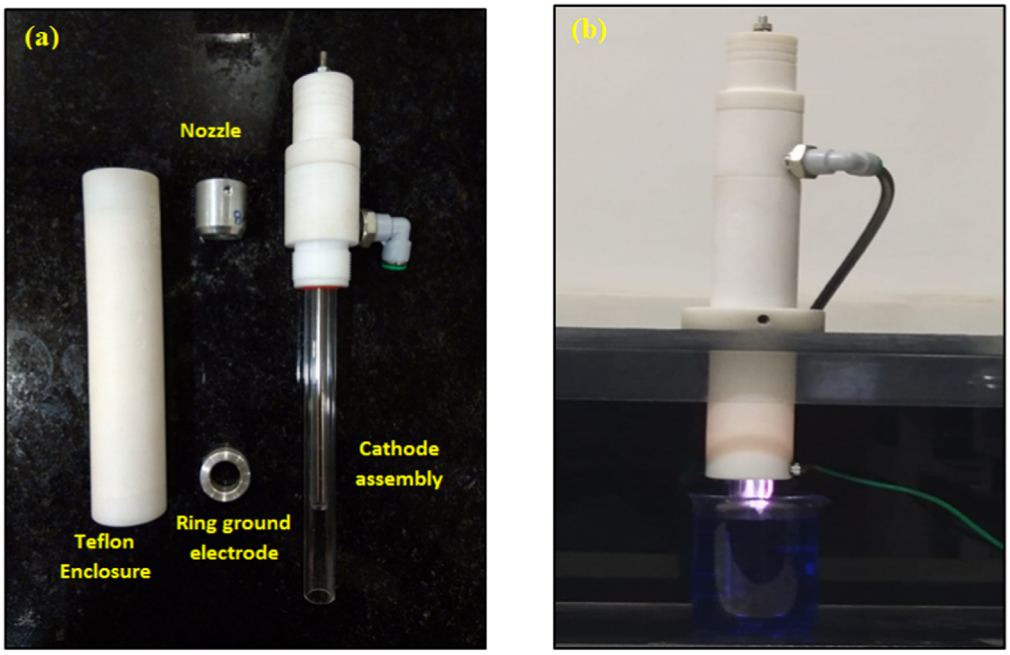


**Figure 1.** Photograph of (a) the torch assembly and (b) plasma jet during processing.

**Table 1.** Critical parameters for RB-198 aqueous solution treatment.

| Parameters | Value |
|---|---|
| Reaction time | 10–30 min |
| Distance between live electrode and ground | 2.5 cm |
| Distance between nozzle orifice and water surface | 5–17 mm |
| Plasma-forming gas | Ar |
| Ar gas flow rate | 9 lpm |
| Applied potential | 28, 30 and 32 kV |

controllers. A reaction chamber is placed underneath the nozzle exit. Before plasma treatment, 40 ml of RB-198 aqueous solution of $10^{-4}$ mole concentration in a petri dish was placed in the reaction chamber such that the liquid surface was 5 mm down the nozzle exit. Figure 1 displays the plasma reactor during the treatment of the RB-198 dye solution. After preliminary arrangements, argon gas was allowed into the plasma torch at a flow rate of 9 lpm. The plasma was initiated by applying a suitable AC voltage to the live cathode so that stable plasma was obtained with the ring electrode grounded. The plasma plume emerging via the nozzle exit interacted with the dye solution. Plasma treatment was carried out as a function of various operating parameters, which are listed in table 1.

### *2.3. Characterization of plasma-treated RB-198*

The reactive species involved in the degradation of RB-198 molecules in aqueous solutions were investigated by an optical emission spectrometer (Ocean Optics HR4000CG-UV-NIR spectrometer). The emission spectra were recorded in the wavelength region of 200–1100 nm with a spectral resolution of 1 nm. The optical signal produced during the process was collected by an optical fiber cable (QP400-2-SR-BX) and the obtained spectra were studied using OceanView spectroscopy software with a graphical user interface.

Degradation of the RB-198 dye was examined via a UV–Vis spectrophotometer (Ocean Optics HR4000CG-UV-NIR spectrometer) equipped with a DT2000 UV–Vis light source. The percentage of degradation was evaluated from the observed reduction in the absorbance peak of the dye at 625 nm after plasma treatment by the following expression [9]:

$$\%\ \text{of degradation} = \frac{A_{\text{bt}} - A_{\text{at}}}{A_{\text{bt}}} \times 100. \tag{1}$$

In the above expression, $A_{\text{bt}}$ and $A_{\text{at}}$ are the intensities of the maximum absorbance peak in the visible region of the RB-198 dye before and after plasma treatment.

The energy yield of the degradation of RB-198 was also evaluated, which afforded the amount of RB-198 degraded per unit energy consumed during the reaction. It could be evaluated as the following equation [9]:

$$Y\left(\frac{\text{g}}{\text{kWh}}\right) = \frac{C\left(\frac{\text{g}}{\text{l}}\right) \times V(\text{l}) \times \frac{1}{100} \times \text{degradation}(\%)}{P(\text{kW}) \times t(\text{h})} \tag{2}$$

where $C$ and $V$ are the initial concentration and volume of RB-198 solution, while $P$ and $t$ are the power and reaction time, respectively.

The pH and conductivity of untreated and plasma-exposed dye solution were monitored by a digital pH meter (Hanna Instruments, USA) and digital electrical conductivity meter-611 (Eloco Ltd, India). The change of total organic carbon (TOC) in the untreated and plasma-exposed RB-198 aqueous solution was determined by a Shimadzu TOC-LPH total organic carbon analyzer.

The concentration of $OH^{\bullet}$ radicals produced in the liquid during plasma treatment was analyzed by chemical dosimetry based on terephthalic acid (TA), which acts as an $OH^{\bullet}$ scavenger that does not react with other radicals and reactive species ($H_2O_2$, $O_2^-$ etc). The $OH^{\bullet}$ radical reacts with TA forming hydroxyterephthalic acid (HTA), which can be identified and determined quantitatively by measuring the fluorescence emission in the visible region [19]. The concentration of HTA formed is directly proportional to the concentration of $OH^{\bullet}$ radicals, and by measuring the intensity of the fluorescence emission, the concentration of $OH^{\bullet}$ radicals can be determined. Before the experiment, TA is added to the aqueous dye solution, which was maintained at a pH of 10 using NaOH because TA is insoluble in acidic and neutral solution. A further 25 ml of the solution in a 50 ml beaker was exposed to a plasma jet and experiments were carried out under various treatment parameters. After that, the plasma-treated solution was further irradiated by a 310 nm UV light source and the resulting fluorescence emission line at 425 nm was observed by spectrophotometer via optical fiber cables [14, 19].

The presence of $H_2O_2$ in the plasma-treated aqueous solution was further examined via a spectrophotometric method involving potassium titanium (IV) oxalate. Initially, 3.54 g of potassium titanium (IV) oxalate ($K_2TiO$ ($C_2O_4$) $2H_2O$) was added into the solution containing 27.2 ml of concentrated sulfuric acid and 30 ml of distilled water. The volume of the obtained solution was increased to 100 ml by adding deionized water (DI) and this titanium reagent was used for determination of the concentration of $H_2O_2$. For spectroscopic measurement, 5 ml of titanium reagent and 5 ml of the dye solution were poured into a calibrated flask the volume of which was increased to 25 ml by the addition of DI water. The obtained solution was further exposed to plasma at various operating parameters. Finally, the absorbance spectra of the plasma-treated and untreated solutions were measured using the spectrophotometer at 400 nm [14]. The presence of $H_2O_2$ was calculated as follows [20]:

$$[H_2O_2] = \frac{(A_{at} - A_{bt})}{37.4\, xl} \tag{3}$$

where $A_{bt}$ and $A_{at}$ are the intensities of the absorbance spectra of untreated and plasma-treated solutions, respectively. $x$ and $l$ are the volume of the solution and path length of the spectrophotometer cuvette (cm).

### 2.4. Toxicity analysis

#### 2.4.1. Seed germination, plant growth and toxicity analysis.

Tomato (Solanum Lycopersicum) seeds were used for this experiment. Seeds (25 seeds) were initially planted in two separate pots containing 100 g of soil. Subsequently, 10 ml of untreated and plasma-treated dye solution (at room temperature) were poured into the cultivation pots for three consecutive days. After three days, the length of the stem of the plants germinated by untreated and plasma-treated dye solution was measured. Moreover, the growth rate of the plant was also examined six days after sowing [21]. The toxicity of the plasma-treated RB-198 aqueous solution was investigated by the agar well diffusion bacterial growth method using *Staphylococcus aureus* (*S. aureus*) and *Escherichia coli* (*E. coli*) bacteria.

## 3. Results and discussion

### 3.1. Investigation of reactive species during plasma treatment: OES results

Before investigating the plasma effect on the degradation of RB-198 aqueous solution, it is important to investigate the information regarding reactive species present in the plasma jet afterglow region and the reactive species formed during plasma treatment. This was examined by means of OES. Before the plasma treatment of RB-198, the plasma is produced at various applied potentials of 28, 30 and 32 kV with the fixed flow rate of 9 lpm, resulting in a plasma plume emerging via the nozzle exit. The emission spectrum of the Ar plasma jet discharging in air (relative humidity 64% and temperature 31 °C) and the spectrum are displayed in figure 2(a).

It was found that the most dominant emission peaks observed in the emission spectra of the Ar plasma excited at 28 kV were due to atomic Ar emission spectral lines, which were obtained at the wavelength region of 695–960 nm [22–27]. Furthermore, we found one small peak at 308.5 nm, attributed to $OH^{\bullet}$ radicals (transition $A^2\Sigma \rightarrow X^2\Pi$), which may be formed by the interaction of plasma with atmospheric oxygen and moisture as it emerges from the orifice of the nozzle. A similar tendency was observed when the plasma was excited at higher applied potentials of 30 and 32 kV. However, the intensities of the emission peaks increased with further increase in the applied potential, as shown in figure 2(a). This may be attributed to the increase in the degree of ionization of plasma, resulting in increased concentration of reactive species of Ar and energetic electrons, which further interact with moisture and oxygen leading to an increase in the concentration of $OH^{\bullet}$ radicals [25–27]. The above results clearly confirm that the most dominant reactive species in the Ar plasma jet was Ar species. In contrast, the OES spectrum of the plasma jet during the degradation of RB-198 at 28 kV shows many new peaks attributed to $N_2$ second positive system (334.03, 354.56 and 376.84 nm) (transition $C^3\Pi_u$-$B^3\Pi_g$), atomic oxygen species (OI at 772.63 and 843.89 nm), nitric oxide (NO) radicals ($A^2\Sigma^+$-$X^2\Pi$, at 206.42, 224.38 and 236.04 nm) and H line of the Balmer series such as $H_\alpha$ (at 656.58 nm), $H_\beta$ (at 486.46) and $H_\gamma$ (at 430.8 nm ) (figure 2(b)) [23–29]. Moreover, the intensities of the existing peaks due to $OH^{\bullet}$ radicals and Ar species increased slightly compared with those of the spectral lines obtained before treatment. The formation in $OH^{\bullet}$ radicals and hydrogen species during the plasma treatment may be attributed to the fragmentation/decomposition of water molecules ($H_2O + e^- \rightarrow OH^{\bullet} + H^{\bullet} + e^-$), whereas the formation of atomic oxygen may be due to the dissociation of oxygen molecules ($O_2 + e^- \rightarrow O + O + e^-$). Moreover, the

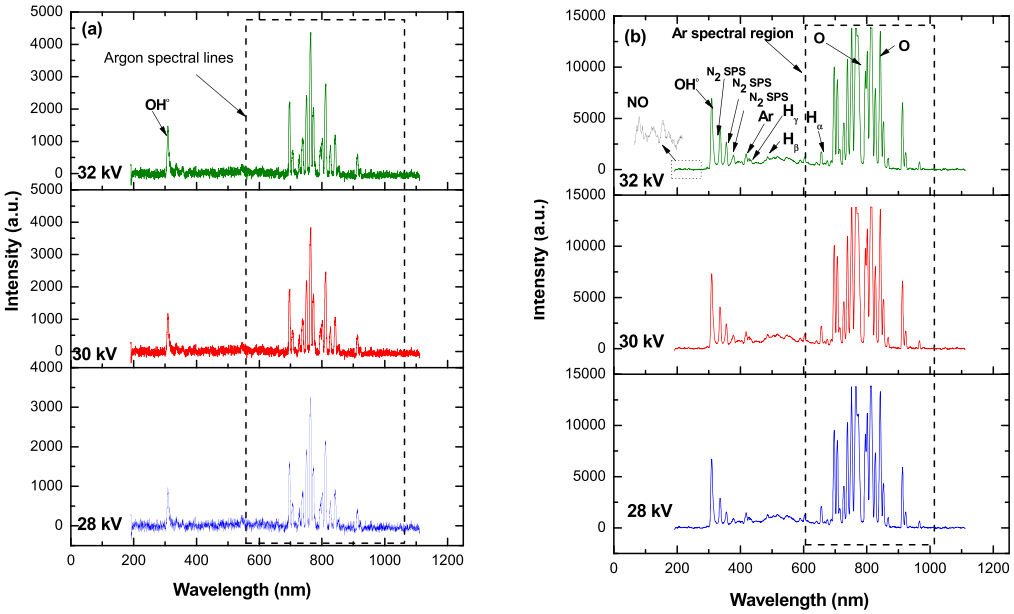


**Figure 2.** OES spectra of Ar plasma jet as a function of applied potential (a) before treatment and (b) during treatment.

formation of nitrogen species in the OES of the plasma jet during treatment of the dye solution is significant and may be due to the breaking down of the dye molecule into simpler molecules and nitrogen, which are excited by reactive species in the plasma ($N_2$ ($X^1\Sigma$) + $Ar^*$ → $N_2$ ($C^3\Pi$) + Ar) [29]. It was recognized that the formation of NO may be due to the interaction of reactive $N_2$ with $O^\bullet$ radicals [28]. Besides, the presence of $N_2$ components may also be attributed to the interaction of ambient air with the plasma at the gas-liquid interface. The intensity of the peaks due to various species was found to gradually increase with increasing applied potentials, as shown in figure 2(b). The above fact may be attributed to the increased density of energetic electrons in the plasma column because of the higher degree of ionization occurring at higher applied potentials. The energetic electrons further interact with the atoms or molecules on the surface of the liquid or in the region between the nozzle and liquid surface, resulting in the formation of various reactive oxygen and nitrogen species (ROS and RNS) as well as UV radiation. The reactive species formed are further transported to the liquid column, leading to the breakdown of RB-198 dye molecules by strong oxidation and degradation of the molecules of the dyes.

### *3.2. Degradation effect of RB-198: UV–Vis spectral results*

The degradation of RB-198 molecules in aqueous solution due to plasma treatment was further studied using a UV–Vis spectrometer by measuring the absorbance at 620 nm corresponding to the maximum absorbance of the dye. The UV–Vis spectra of the untreated RB-198 solution exhibits a clear absorption peak in both UV and visible regions of wavelength at 277 and 620 nm due to anthraquinone structure and blue color of the chromophore of RB-198, respectively (figure 3(a)) [30, 31].

The intensity of both absorbance peaks decreased sharply even at short exposure time of 10 min at 28 kV applied potential and the intensity of the peaks further decreased with increasing reaction time, as shown in figure 3(a). The decoloration of RB-198 aqueous solution was further studied by treating the solution at higher applied potentials and reaction times. The results are similar to those obtained at lower applied potential of 28 kV. However, complete degradation was obtained at higher applied potential and reaction time (figures 3(b) and (c)). Figure 4 reveals the variation in the percentage of degradation of RB-198 dye molecules for different operating conditions. The percentage of degradation of the dye molecules was observed to be 97% for the first 10 min of reaction time at 28 kV and further increased with increasing reaction time (figure 4). After increasing the applied potential, a similar tendency was observed for various reaction times. Nevertheless, the maximum degradation rate was found to be obtained for the sample treated at higher reaction time of 30 min and an applied potential of 32 kV (99.27%). The variation in the rate of degradation process is mainly due to the production of higher concentration of ROS and RNS along with higher intensity of UV radiation generated at higher applied potentials. The results show direct correlation of plasma parameters, concentration of reactive species and extent of dye degradation.

The higher concentration of plasma-generated reactive species as well as the higher intensity of UV radiation at higher applied potential facilitated the destruction of the RB-198 dye molecules in the aqueous solution at a faster rate compared to the degradation rate at lower potential. Furthermore, the generation of reactive species as well as the emission of photons is actually proportional to the reaction time and because of this, the rate of the degradation process increases with increasing reaction time. However, the time required for complete degradation of the dye decreased at increased applied potential due to the formation of higher

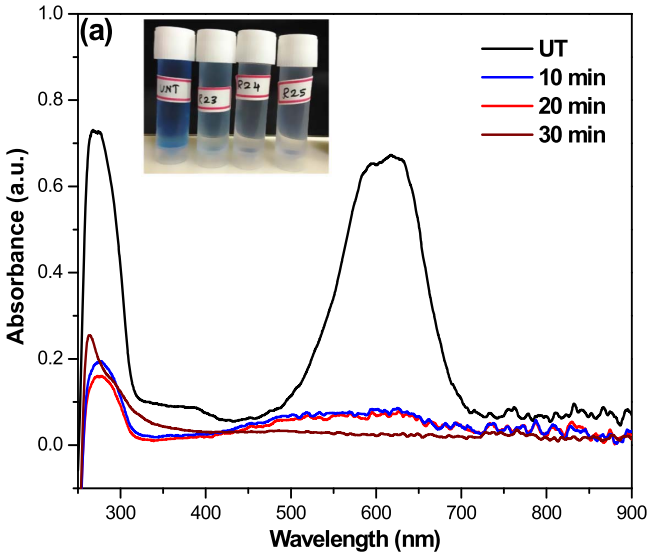


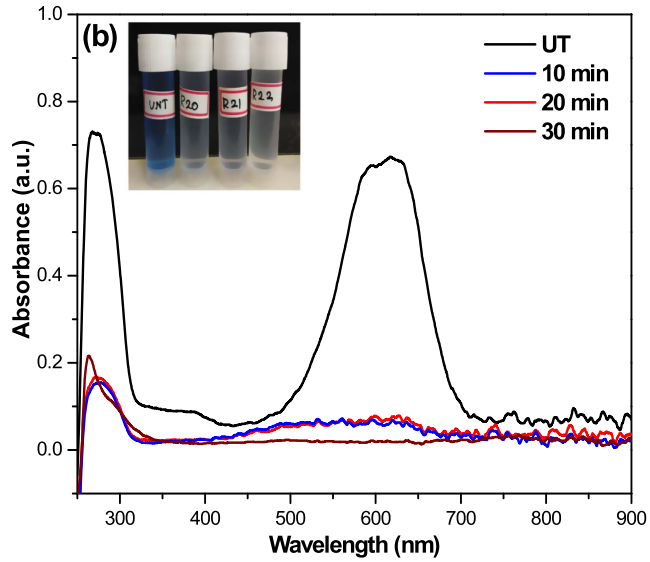


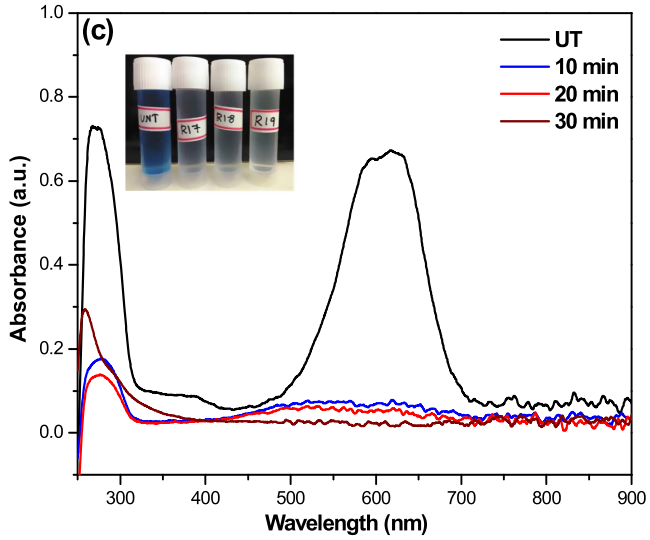


**Figure 3.** UV–Vis absorbance spectra of plasma-treated RB-198 aqueous solution as a function of reaction time and applied potentials (a) 28, (b) 30 and (c) 32 kV.

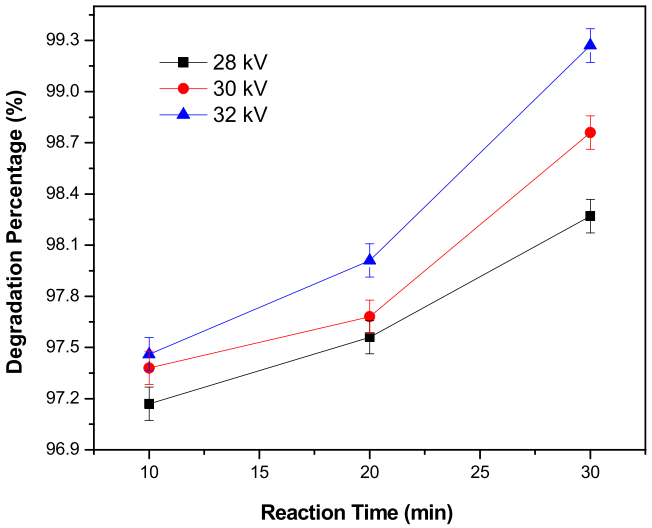


**Figure 4.** Variation of the percentage of degradation of RB-198 aqueous solution as a function of reaction time and applied potential.

concentration of reactive species. Furthermore, figure 5(a) shows the variation of absorbance spectra of the plasma-treated RB-198 aqueous solution as a function of distance between the plasma exit and water surface. It was found that the intensity of the absorbance spectra due to the anthraquinone and chromophore of RB-198 decreases with decreasing the distance between the nozzle orifice and water surface. This is due to increased interaction of the plasma jet with the dye solution when the plasma jet was closer to the liquid surface. The results are further confirmed by the variation in percentage of degradation with distance between the nozzle orifice and liquid surface, as displayed in figure 5(b).

It is evident from the figure that the percentage of degradation increases with decreasing the distance between the plasma jet and liquid surface. This is due to the fact that the reactive species formed during the reaction are easily transported to the solution when the jet is placed very close to the surface of the liquid, whereas when the distance between the nozzle and liquid surface increases, most of the reactive species lose their energy by various collision processes, resulting in the suppression of dye degradation [32]. From the above results, we confirm that the degradation of RB-198 molecules highly depends on the plasma operating parameters and concentration of reactive species.

### *3.3. Energy yield*

Figure 6 shows variation in energy yield as a function of various operating parameters. It was observed that energy yield decreased gradually with increasing the reaction time at the applied potential of 28 kV. The decrease in energy yield with respect to reaction time may be due to consumed higher extent of energy for longer reaction time, resulting in decreasing energy yield, but increasing percentage of degradation of RB-198 aqueous solution [9, 16, 33]. A similar trend was observed at the RB-198 treated at higher applied

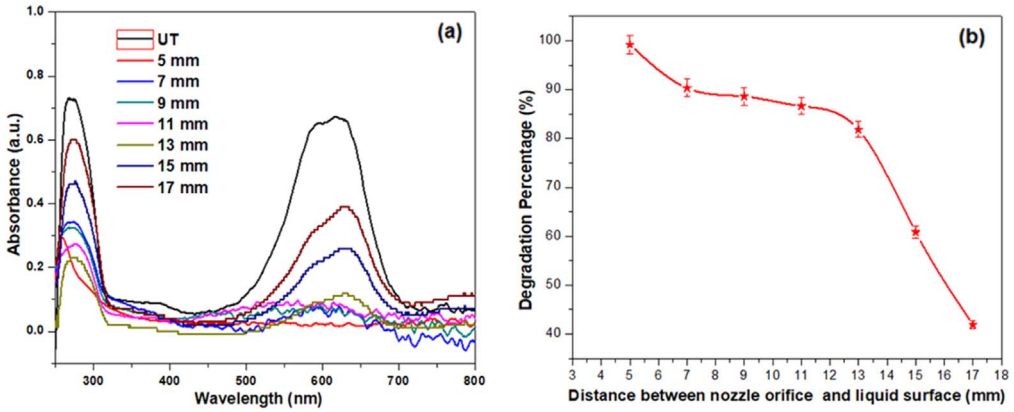


**Figure 5.** (a) UV–Vis absorbance spectra of and (b) degradation (%) of plasma-treated RB-198 aqueous solution as a function of the distance between the nozzle orifice and liquid surface ($t = 30$ min and $V = 32$ kV).

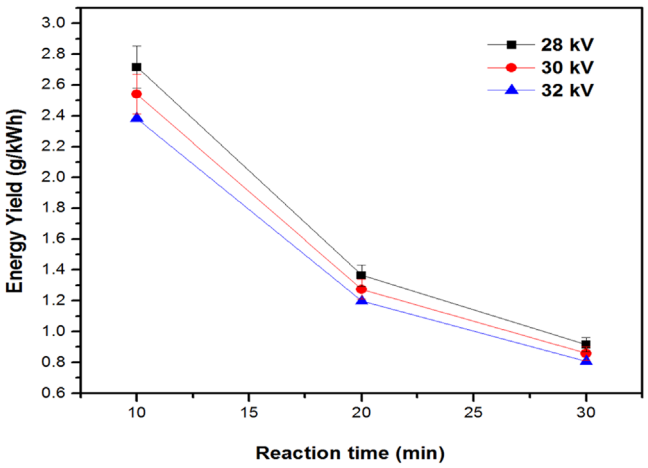


**Figure 6.** Energy yield as a function of reaction time and applied potential.

potentials of 30 and 32 kV, respectively. Among them, RB-198 treated at higher potential and reaction time of 32 kV and 30 min, respectively, exhibits very low energy yield, whereas it obtained higher degradation (%) compared with other operating parameters.

### *3.4. Evaluation of reactive species*

The concentration of $OH^{\bullet}$ radicals produced in the liquid during plasma treatment was analyzed by chemical dosimetry based on TA, which forms HTA. The concentration of HTA is determined by measuring the intensity of fluorescent emission at 425 nm. In general, the TA molecules do not react with other oxygen species ($O_3$ and $H_2O_2$) and hence TA molecules alone will not produce fluorescent emission at 425 nm [14, 33].

However, it can produce fluorescent emission when it interacts with $OH^{\bullet}$ radical by the formation of highly fluorescent HTA. The concentration of $OH^{\bullet}$ radical in aqueous solution is acquired by measuring the intensity of the fluorescent emission because the intensity of the fluorescence emission is directly proportional to the concentration of $OH^{\bullet}$ radicals. Figure 7(a) presents the fluorescence emission intensity of HTA solution after plasma exposure at different applied potentials and reaction times. It can be seen that the intensity of fluorescence emission increases gradually with increasing reaction time when the treatment was carried out at 28 kV of applied potential. A similar tendency was observed in the case of the aqueous dye solution treated at higher potentials of 30 and 32 kV. However, the higher emission intensity was observed for aqueous solutions treated at higher potential and reaction time (32 kV and 30 min). A possible reason for the above changes in formation of $OH^{\bullet}$ radicals in aqueous solution may be due to the following facts: when extending reaction time, the reactive plasma species get more time to interact with molecules of aqueous solution giving rise to the formation of higher density of $OH^{\bullet}$ radicals. At higher applied potential, the degree of ionization of plasma gas is very high, which leads to the production of higher concentration of reactive species such as excited Ar species, electrons, excited oxygen atoms, photons and $N_2$ under second positive system that strongly interact with water molecules in aqueous dye solution, resulting in the formation of higher concentration of $OH^{\bullet}$ radicals by the following reaction [34–37]:

$$H_2O + e^- \rightarrow OH^{\bullet} + H^{\bullet} + e^- \quad \text{(R1)}$$

$$O + H_2O \rightarrow 2OH^{\bullet} \quad \text{(R2)}$$

$$N_2{}^* + H_2O \rightarrow OH^{\bullet} + N_2 + H \quad \text{(R3)}$$

$$H_2O + e^- \rightarrow OH^{\bullet} + H^- \quad \text{(R4)}$$

$$Ar^* + H_2O \rightarrow OH^{\bullet} + H + Ar \quad \text{(R5)}$$

$$H_2O + h\upsilon \rightarrow OH^{\bullet} + H^{\bullet} \quad \text{(R6)}$$

Figure 7(b) shows the variation of fluorescent emission intensity as a function of the distance between the nozzle orifice and liquid surface. It exhibits that the intensity of the fluorescent emission peak decreases with increasing distance between the plasma jet and water surface. Thus, the transportation of plasma species into the liquid may be decreased with the increase of distance between the nozzle orifice and water surface, i.e. most of the reactive species lose their energy by either elastic or inelastic collisions with air molecules present in the region between the plasma jet and liquid surface, resulting in suppression of the formation of $OH^{\bullet}$ radicals on the water surface.

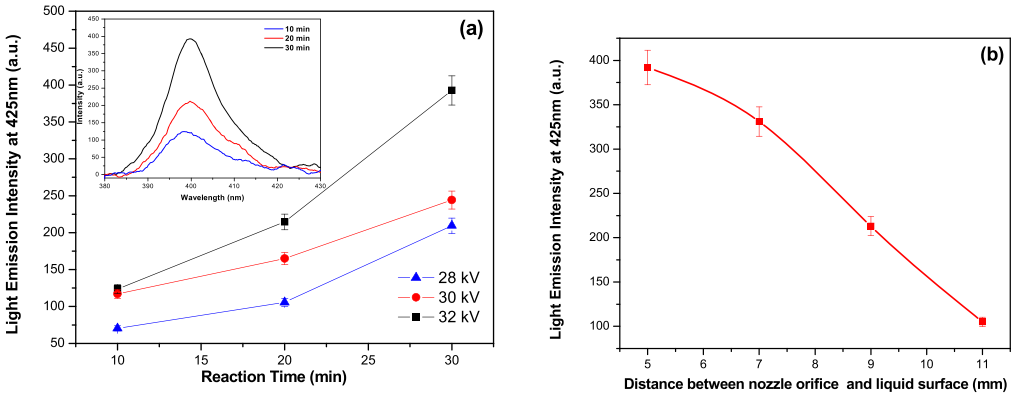


**Figure 7.** Fluorescence analysis of $OH^{\bullet}$ radicals as a function of (a) reaction time and applied potential, (b) distance between the nozzle orifice and liquid surface (mm) using TA solution.

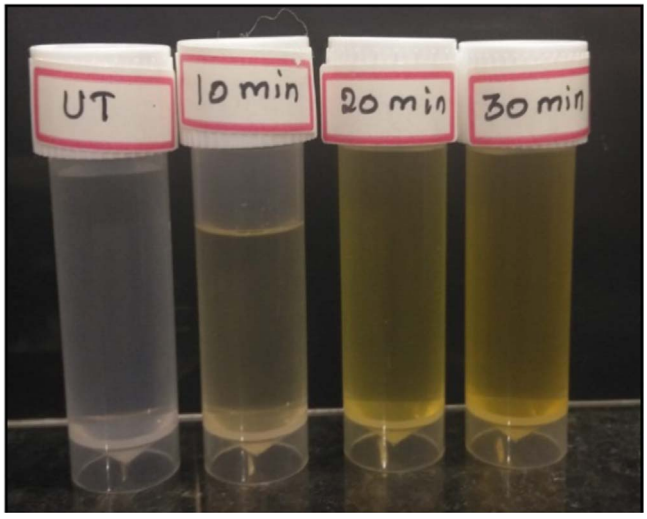


**Figure 8.** Photograph of the reaction of plasma-treated aqueous solution with potassium titanium (IV) oxalate (PTO) solution.

The concentration of $H_2O_2$ in the plasma-treated water was further studied by spectrophotometric evaluation using potassium titanium (IV) oxalate (PTO) because it reacts with the $H_2O_2$ in water solution to produce a yellowish-orange color [20]. Figure 8 shows the color variation of plasma-treated aqueous solution after reaction with PTO. It can be evidently seen that the color of the untreated water after PTO addition exhibits a white color due to the absence of $H_2O_2$ in the liquid. However, the addition of PTO to dye solution exposed to plasma for 10 min ($V = 32$ kV) produces a light yellowish-orange color due to the generation of $H_2O_2$ in the solution by plasma treatment. The color of the solution intensified with increasing reaction time due to the generation of higher concentration of $H_2O_2$, which was further studied spectroscopically by determining the absorption peak with the maximum wavelength of 400 nm.

Figure 9(a) shows the variation of $H_2O_2$ concentration in plasma-treated dye solution as a function of various operating parameters such as reaction time and applied potential. It clearly exhibits that the concentration of $H_2O_2$ gradually increases with increasing reaction time at fixed applied potential of 28 kV, which indicates an increased production rate of $H_2O_2$ with respect to reaction time. A similar trend was observed when the sample was treated at higher applied potentials of 30 and 32 kV. However, the concentration of $H_2O_2$ was found to be higher for the dye solution treated at higher applied potential and reaction time, as shown in figure 9(a). As the applied potential increases, the $H_2O_2$ production rate was also enhanced, as shown in figure 10(a). The generation of $H_2O_2$ may be due to high electron density, plasma energy and long-lived excited species that aided the transfer of energy between excited species and water molecules, leading to the formation of $H_2O_2$ [20, 33–36]. Moreover, atomic oxygen O can also interact with water molecules to form $H_2O_2$. The mechanism of the formation of $H_2O_2$ in aqueous solution might be as follows [36, 37]:

$$OH^{\bullet} + OH^{\bullet} \rightarrow H_2O_2 \quad \text{(R7)}$$

$$OH^{\bullet} + OH^{\bullet} + Ar^{*} \rightarrow H_2O_2 + Ar \quad \text{(R8)}$$

$$O + H_2O \rightarrow H_2O_2 \quad \text{(R9)}$$

Figure 9(b) exhibits the change in the formation of $H_2O_2$ in the aqueous solution as a function of distance between the plasma jet and liquid surface. It is shown that the formation of $H_2O_2$ decreased with increasing distance between the nozzle orifice and water surface at constant applied potential ($V = 32$ kV) and reaction time (30 min). Also, figure 10(b) shows that the production rate of $H_2O_2$ was found to decrease with increasing the distance between the nozzle orifice and water surface. This may be due to lower concentration of $OH^{\bullet}$ radicals in the liquid surface, resulting in decrease in $H_2O_2$ formation. Thus, with increase of distance between the nozzle orifice and water surface, the number of plasma species transported into the liquid may decrease due to inter-species collision that results in a large fraction of the reactive species losing their energy when they reach the aqueous medium. This results in suppression of the formation of $OH^{\bullet}$ radicals on the water surface and consequently, the concentration of $H_2O_2$ decreases. Finally, we conclude that $H_2O_2$ formation is highly dependent on the formation of $OH^{\bullet}$ radicals and the results of $H_2O_2$ formation are in good agreement with $OH^{\bullet}$ radical concentration. Furthermore, it is also possible to produce reactive nitrogen species such as nitric oxide, nitrogen dioxide and nitrogen radicals (NO, $NO_2$ and $N^{\bullet}$) during the reactions, which are thereafter converted into $NO_3^-$ and

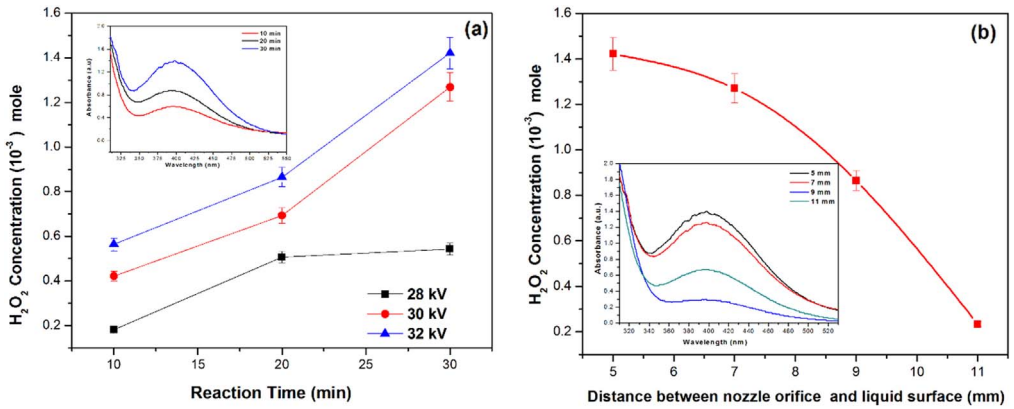


**Figure 9.** $H_2O_2$ concentration as a function of (a) reaction time and applied potential, (b) distance between the nozzle orifice and liquid surface (mm).

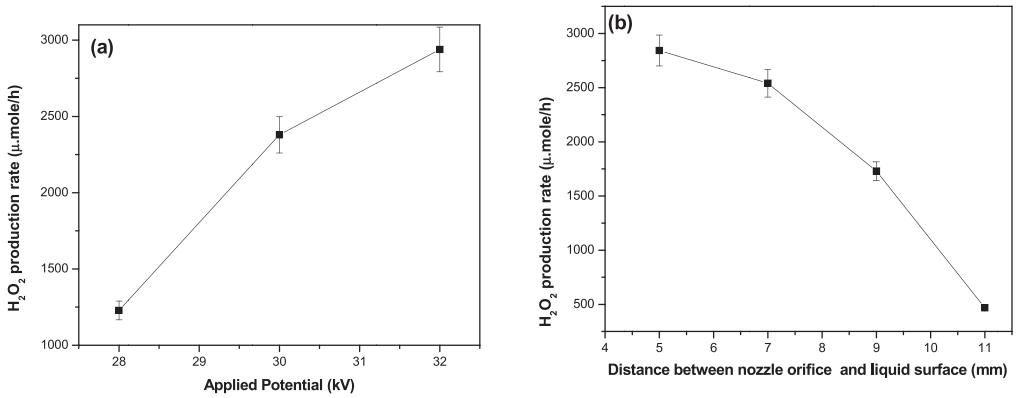


**Figure 10.** $H_2O_2$ production rate as a function of (a) applied potential, (b) distance between the nozzle orifice and liquid surface (mm) at 32 kV.

$NO_2^-$ by the following mechanism [37–39]:

$$N_2 + e \rightarrow N^{\bullet} + N^{\bullet} \quad \text{(R10)}$$

$$N^{\bullet} + O_2 \rightarrow NO + O^{\bullet} \quad \text{(R11)}$$

$$NO + O_3 \rightarrow NO_2 + O_2 \quad \text{(R12)}$$

$$NO_2^- + 2OH^{\bullet} \rightarrow NO_3^- + H_2O \quad \text{(R13)}$$

$$NO_2 + OH^{\bullet} \rightarrow HNO_3 \rightarrow H^+ + NO_3^- \quad \text{(R14)}$$

$$NO + OH^{\bullet} \rightarrow HNO_2 \rightarrow H^+ + NO_2^- \quad \text{(R15)}$$

The formation of RNS is confirmed by variation in pH and electrical conductivity of the solution, which is described in detail in section 3.5. From the above results, we concluded that the plasma-induced generation of $OH^{\bullet}$ radicals and $H_2O_2$ plays a vital role in the degradation of molecules of RB-198 in aqueous solution.

### *3.5. TOC, pH and conductivity measurements*

The mineralization of the RB-198 components in the aqueous solution was further evaluated by measuring the TOC in the plasma-treated solution. Figure 11(a) depicts the variation of the percentage of TOC removed from the dye solution as a function of reaction time and applied potential. It is observed that the TOC-removal percentage from the RB-198 solution treated for 10 min at 28 kV was 17.7%; furthermore, the percentage of TOC removal was observed to increase with increasing reaction time. A similar trend was observed when the applied potential was increased to 30 kV. On further increasing the applied potential to 32 kV, about 80% TOC could be removed from the RB-198 aqueous solution within 20 min of the reaction time and thereafter no significant change was observed at higher reaction time of 30 min. The increase in TOC-removal percentage was mainly due to the mineralization of components of RB-198 molecules in the aqueous solution by plasma treatment [40–42]. Furthermore, the percentage of TOC removal gradually decreased with increasing the distance of the plasma jet orifice from the water surface (figure 11(b)), which may be attributed to loss of energy of the plasma particles before they reach the reaction site, which leads to a decrease in degradation of the RB-198 molecules in aqueous solution.

The measurement of the pH of the plasma-treated solution is one of the direct indicators of mineralization or oxidation of organic content in the solution. Table 2 lists the variation in pH of the plasma-treated RB-198 aqueous solution with respect to various operating parameters. It is shown that the pH value of the untreated RB-198 aqueous solution was 7.5 and decreased gradually with increasing the plasma reaction time at a constant applied potential of 28 kV. A similar tendency was observed at increased applied potentials.

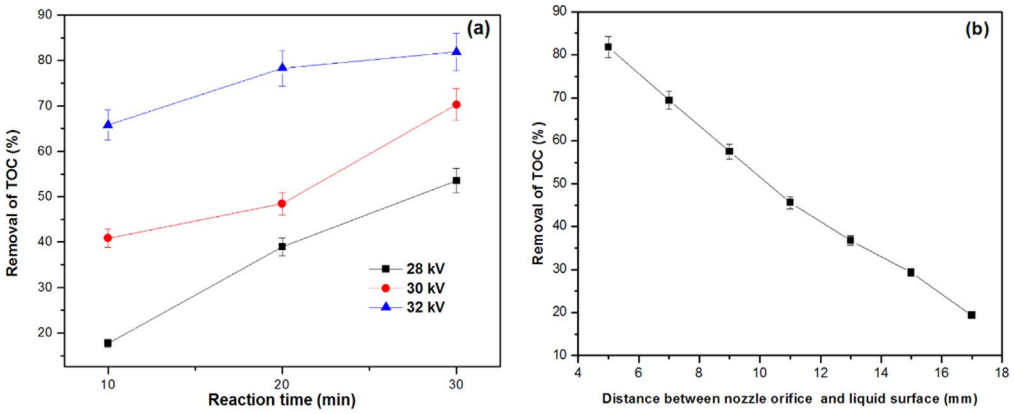


**Figure 11.** Removal of TOC (%) as a function of (a) reaction time and applied potential, (b) distance between the nozzle orifice and liquid surface (mm) at 32 kV.

**Table 2.** Variation of pH, and electrical conductivity of plasma-treated RB-198 aqueous solution for various operating parameters.

| Applied potential (kV) | Reaction time (min) | Distance between nozzle orifice and water surface (mm) | pH | Electrical conductivity ($\mu$S cm$^{-1}$) |
|---|---|---|---|---|
| 28 | 0 | 5 | 7.5 | 0.14 |
| | 10 | | 6.8 | 0.18 |
| | 20 | | 5.6 | 0.19 |
| | 30 | | 4.9 | 0.21 |
| 30 | 10 | 5 | 6.3 | 0.18 |
| | 20 | | 5.2 | 0.20 |
| | 30 | | 4.6 | 0.22 |
| 32 | 10 | 5 | 5.4 | 0.19 |
| | 20 | | 4.6 | 0.22 |
| | 30 | | 3.4 | 0.24 |
| 32 | 30 | 5 | 3.4 | 0.24 |
| | | 7 | 4.8 | 0.22 |
| | | 9 | 5.1 | 0.21 |
| | | 11 | 5.3 | 0.19 |
| | | 13 | 5.4 | 0.18 |
| | | 15 | 6.0 | 0.17 |
| | | 17 | 6.5 | 0.15 |

However, in the case of samples treated at higher applied potential and reaction time, the pH value is found to drop to about 3.4. Furthermore, the solution exhibits a lower pH value when the nozzle orifice is located much closer to the liquid surface (5 mm) than the pH values of samples kept at larger distances from the nozzle orifice (table 2). The above changes may be due to the formation of acids such as nitric acid, sulfonic acid, hydrocholoric and chloro acrylic acid as a consequence of the breakdown and oxidation of dye molecules during the plasma treatment [42–44]. Table 2 also lists the changes in conductivity of the plasma-treated RB-198 solution as a function of reaction time and potential. It is found that the conductivity of the untreated solution was 0.14 $\mu$S cm$^{-1}$ and was further increased with increasing reaction time at fixed applied potential of 28 kV. Finally, the maximum conductivity was observed for the sample treated at higher reaction time, higher applied potential and plasma jet positioned closer to the liquid surface. The increase in conductivity may be attributed to the formation of higher concentration of ionic species such as $Cl^-$, $HCO_3^-$, $NO_2^-$ and $NO_3^-$ in the liquid during processes [45–47].

### 3.6. Toxicity analysis

*3.6.1. Diffusion bacterial analysis.* The toxicity of the plasma-treated RB-198 aqueous solution was studied by examining the growth of bacteria such as *S. aureus* and *E. coli*. The toxicity analysis was carried out on the sample treated at higher applied potential (32 kV) for various reaction times. Figure 12 depicts the growth and proliferation of bacteria in the plasma-treated RB-198 aqueous solution. It was observed that there was no bacterial growth on the site of the untreated liquid, which exhibits a clear inhibition zone, as shown in the figure. This is due to the presence of RB-198 components in the solution, which exhibits toxicity against the bacteria, resulting in the suppression of growth and proliferation of bacteria on the untreated site.

In contrast, all the plasma-treated liquid sites had been completely covered by bacteria due to substantial growth and proliferation of the bacterial colony, which indicates non-toxic properties of plasma-treated water. These results clearly confirm that the components of toxic RB-198 molecules are completely decomposed by the plasma treatment, which revealed significant non-toxic properties [48].

*3.6.2. Seed germination and plant growth.* The non-toxicity of plasma-treated water was further studied by the germination of tomato seeds and the results are portrayed in figure 13. This confirms that most of the sown seeds grow under very healthy conditions. Furthermore, the growth density is remarkable in the case of plants watered with plasma-treated dye solution (figures 13(a) and (b)).

Moreover, the seeds grown using plasma-treated solution exhibited 50% additional growth rate compared with that of using untreated solution, as can be seen in figure 13(c). The above toxicity analysis clearly demonstrates the non-toxic behavior of the plasma-treated solution towards bacterial

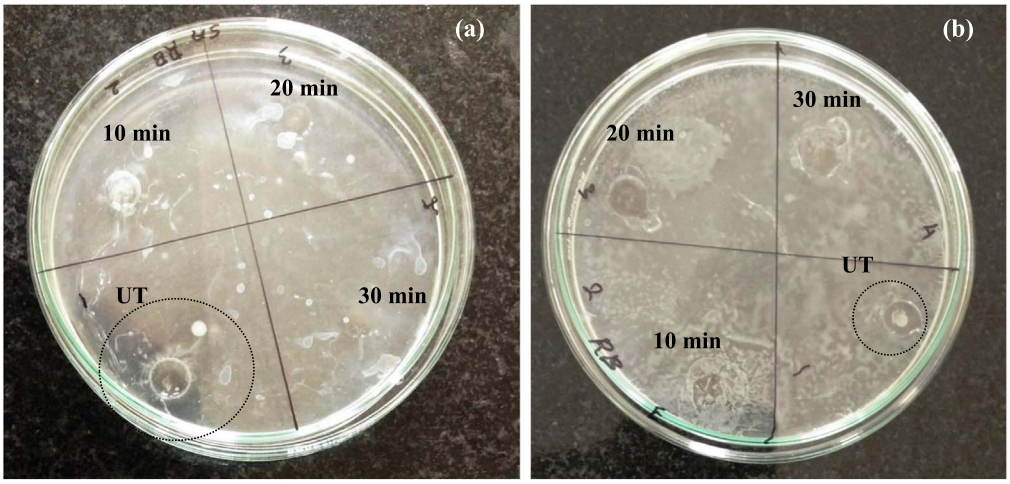


**Figure 12.** Photograph of the estimation of the antibacterial effect of RB-198 aqueous solution as a function of reaction time (at 32 kV) against (a) *S. aureus* and (b) *E. coli* strains.

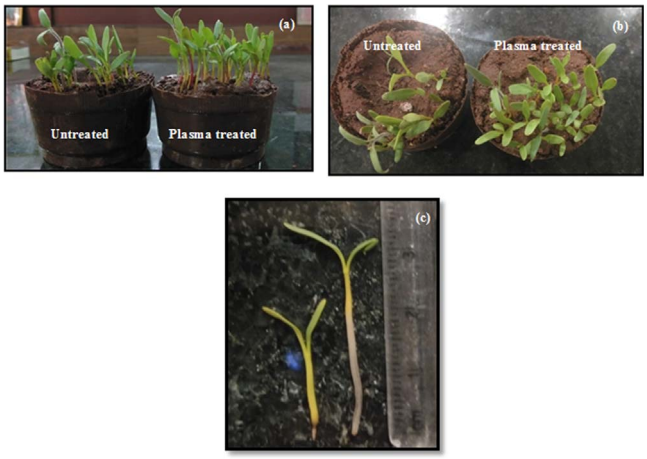


**Figure 13.** Photograph of the growth of plants using untreated and plasma-treated RB-198 solution: (a) cross-sectional view, (b) top view, (c) yield of tomato seedlings on the 3rd day after seeding.

growth and germination of seeds due to destruction of the dye components. Furthermore, the presence of ROS and RNS in the plasma-treated water is an important factor to enrich the germination of seeds [21, 22]. Finally, we conclude that plasma technology has more potential in textile industry applications. Certainly, plasma-treated water has potential applications in agriculture; although additional studies may be required to confirm its use for the irrigation of edible plants, the currently available studies indicate that plasma technology can be used for recycling wastewater for garden applications.

## 4. Conclusion

This paper describes the influence of various plasma operating parameters on the degradation of RB-198 components in simulated dye solution. Various characterization techniques have been used to examine the degradation of plasma-treated samples. Results of experiments indicate that applied potential, exposure time and the nearness of the plasma jet to the water surface significantly affect the degradation of the dye. Degradation of the dye was highest at exposure time of 30 min, applied potential of 32 kV and when the plasma jet was positioned very close to the liquid surface (5 mm) as confirmed by UV–Vis spectra. The OES results exhibit the generation of various reactive species such as $O_3$, $OH^{\bullet}$, $N_2$ SPS and NO during the treatment. The pH, conductivity and TOC results show significant variation with respect to operating parameters and indicate substantial degradation of RB-198 molecules. Analysis of the optical emission spectroscopic data confirms the presence of $OH^{\bullet}$ and $H_2O_2$ in the plasma-treated aqueous solution and was found to increase with an increase in the applied potential and reaction time, and shorter distance between the nozzle orifice and water surface. The presence of nitrogen species indicates that the dye molecules are broken down into simpler compounds and nitrogen gas. The bacterial growth, seed germination and seed growth results reveal the non-toxic nature of the plasma-treated solution due to the degradation of complex and toxic dye molecules to simpler non-toxic components. Finally, we suggest that the plasma-based water treatment has potential in effluent treatment technology, which is an efficient alternative method for conventional AOP techniques.

## Acknowledgments

The corresponding author Dr K N Pandiyaraj would like to express his sincere gratitude to DST-SERB, Government of India for providing the financial support (EMR/2016/006812 Dated: 02-Nov-2017). Dr M Pichumani would like to thank The Management, Sri Ramakrishna Engineering College, Coimbatore, India and Government of India—DST INSPIRE Project 04/2013/000209.

## References


[1] Hayashi Y *et al* 2014 *Jpn. J. Appl. Phys.* **53** 010212
[2] Wang T C *et al* 2016 *Environ. Sci. Pollut. Res.* **23** 13448
[3] Jiang B *et al* 2013 *Chem. Eng. J.* **215–216** 969
[4] Reyes P *et al* 1999 *Biotechnol. Lett* **21** 875
[5] Nguyen V C, Nguyen N L G and Pho Q H 2015 *Adv. Nat. Sci. Nanosci. Nanotechnol.* **6** 035001
[6] Yang X F *et al* 2015 *Appl. Catal.* B **166–167** 231
[7] Watharkar A D *et al* 2015 *J. Hazard. Mater.* **283** 698
[8] Yan J J *et al* 2015 *J. Hazard. Mater.* **283** 730
[9] Manoj Kumar Reddy P, Mahammadunnisa S and Subrahmanyam C 2014 *Indian J. Chem.* **53A** 499
[10] Nikiforov A Y 2009 *IEEE Trans. Plasma Sci.* **37** 872
[11] Gerrity D *et al* 2010 *Water Res.* **44** 493
[12] Magureanu M, Bradu C and Parvulescu V I 2018 *J. Phys. D Appl. Phys.* **51** 313002
[13] Song W *et al* 2019 *J. Environ. Sci.* **83** 1–7
[14] Jamroz P, Dzimitrowicz A and Pohl P 2018 *Plasma Process Polym.* **15** 1700083
[15] Attri P *et al* 2016 *Sci. Rep.* **6** 34419
[16] Rahimpour M *et al* 2019 *J. Environ. Chem. Eng.* **18** 103220
[17] Wang X J *et al* 2019 *Chemosphere* **232** 462
[18] Hentit H *et al* 2014 *J. Mol. Catal. A Chem.* **390** 37
[19] Page S E, Arnold W A and McNeill K 2010 *J. Environ. Monit.* **12** 1658
[20] Sellers R M 1980 *Analyst* **105** 950
[21] Sivachandiran L and Khacef A 2017 *RSC Adv.* **7** 1822
[22] Kim Y H *et al* 2014 *Plasma Chem. Plasma Process.* **34** 457
[23] National Institute of Standard and Technology (NIST Database) (https://physics.nist.gov/PhysRefData/Handbook/periodictable.htm)
[24] Shaw P *et al* 2018 *Sci. Rep.* **8** 11268
[25] Attri P *et al* 2015 *Sci. Rep.* **5** 9332
[26] Barkhordari A *et al* 2017 *J. Theor. Appl. Phys.* **11** 301
[27] Onyshchenko I *et al* 2015 *Plasma Processes Polym.* **12** 466
[28] Jamróz P *et al* 2014 *Plasma Chem. Plasma Process.* **34** 25
[29] Rezaei F *et al* 2018 *Plasma Processes Polym.* **15** 1700226
[30] Rajkumar K and Muthukumar M 2017 *Int. J. Environ. Sci. Nat. Res.* **1** 555570
[31] Rajkumar D, Song B J and Kim J G 2007 *Dyes Pigm.* **72** 1
[32] Kanazawa S *et al* 2012 *Int. J. Plasma Environ. Sci. Technol.* **6** 166
[33] Manoj Kumar Reddy P and Subrahmanyam C 2012 *Ind. Eng. Chem. Res.* **51** 11097
[34] García M C *et al* 2017 *Chemosphere* **180** 239
[35] Sun Y *et al* 2016 *Chemosphere* **155** 243
[36] Zhou R W *et al* 2016 *Sci. Rep.* **6** 39552
[37] Wang T C *et al* 2016 *J. Hazard. Mater.* **302** 65
[38] Huang F M *et al* 2010 *Chem. Eng. J.* **162** 250
[39] He B B *et al* 2017 *J. Phys. D: Appl. Phys.* **50** 445207
[40] Mizuno A 2013 *Catal. Today* **211** 2
[41] Wang J *et al* 2016 *Chem. Eng. J.* **300** 36
[42] De Brito Benetoli L O *et al* 2012 *J. Hazard. Mater.* **237–238** 55
[43] Locke B R *et al* 2006 *Ind. Eng. Chem. Res.* **45** 882
[44] Tang Q *et al* 2009 *Plasma Chem. Plasma Process.* **29** 291
[45] Magureanu M *et al* 2013 *Plasma Chem. Plasma Process.* **33** 51
[46] Matinzadeh Z *et al* 2017 *J. Theor. Appl. Phys.* **11** 97
[47] Lukes P *et al* 2005 *J. Phys. D Appl. Phys.* **38** 409
[48] Bansode A S *et al* 2017 *Chemosphere* **167** 396